Inorganic Chemistry

Article

pubs.acs.org/IC

Electrochemical and Fluorescent Ferrocene-Imidazole-Based Dyads as Ion-Pair Receptors for Divalent Metal Cations and Oxoanions

María Alfonso, Arturo Espinosa Ferao, Alberto Tárraga,* and Pedro Molina*

†Departamento de Química Orgánica, Facultad de Química, Campus de Espinardo, Universidad de Murcia, E-30100 Murcia, Spain

Supporting Information

ABSTRACT: In the tricyclic bis(heteroaryl)substituted ferrocenyl-imidazo-quinoxalines **7** and **8**, the presence of redox and fluorescent units at the heteroaromatic core, which can act as a ditopic binding site, made these molecules potential candidates as electro-optical ion-pair recognition receptors. In this context, both molecules behave as ion-pair receptors for cations and anions, which individually had demonstrated their ability to form the corresponding cationic and anionic complexes. These receptors also show an important enhancement of anion binding by co-bound cations, whereas no affinity of the free receptors by the anion is observed. Similarly, receptors **7** and **8** display a dramatic increase in the cation binding by the action of their anionic complexes, while no affinity of the free receptors by the cations was detected. Interestingly, both receptors exhibit a remarkable enhancement of anions and cations binding, although no affinity of the free receptors by the ions is observed. In all cases, the ion-pair formation is detected by a perturbation of the redox potential of the ferrocene moiety and a remarkable enhancement in the emission band.

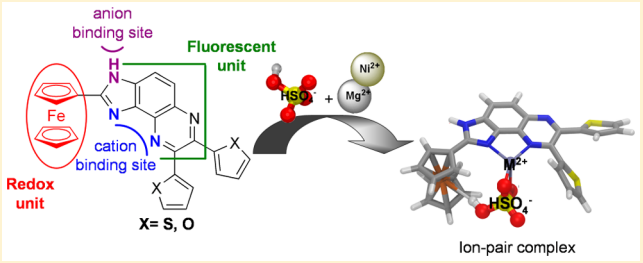

INTRODUCTION

Over the past decade, one of the most vigorous fields of research, within the area of supramolecular chemistry, has been the design and application of new preorganized heteroditopic hosts that are capable of simultaneously sensing both cationic and anionic guests, that is, ion-pair recognition receptors.[1]

Among the receptors designed to form ion-pair complexes, multidentate N- or O-ligands (e.g., crown ether moieties) and electron-rich aromatic rings have been extensively used as the cation binding sites,[2] while the ways used for binding anions are based on Lewis acidic, electrostatic, or hydrogen bonding interactions.[3] Such systems are interesting, not only as switches[4] but also for molecular sensing.[5] Although a variety of approaches have been reported to be effective for binding of ion pairs, the number of well-characterized receptors that bind concurrently both cations and anions still remains scarce.

The ferrocene unit is the most popular among the redox signaling motif currently being used for the incorporation into suitable receptors to bind cations, anions and neutral molecules and allow their electrochemical sensing. It is worth mentioning that, in the ferrocene-containing ligands bearing the recognition sites close to the redox function, the cation binding induces a positive shift in the redox potential of the ferrocene/ferrocenium redox couple, while significant cathodic shifts are observed when complexed to an anion. Thus, preparation and sensing properties of ferrocene derivatives have been comprehensively reviewed.[6]

One approach to the design of small-molecule-based ion-pair receptors is based on the use structural motifs containing the imidazole ring because, due to its amphoteric nature, it behaves as an excellent hydrogen bond donor moiety, allowing the acidity of the NH proton to be tuned by changing the electronic properties of the imidazole substituents. Even more, imidazole ring shows the peculiarity of having a donor pyridine-like nitrogen atom within the ring, capable of selectively binding cationic species, which also converts the imidazole-containing derivatives into excellent metal ion sensors.[7] In this context, the use of ferrocenyl-imidazole receptors could be a valuable strategy for the electrochemical detection of anions or cations. Consequently, several examples of such receptors have been successfully reported as chemosensors for different types of ions.[8]

On the other hand, quinoxalines[9] represent a well-known class of fluorescent compounds with high quantum yields displaying a high potential for special and high-technology applications. Thus, fluorescent ion sensors bearing quinoxalines fused to additional azaheterocyclic units that allow the recognition of anions[10] and cations[11] have recently been reported.

In this context, we herein report on the synthesis, characterization, and binding abilities for cations, anions, and ion pairs of the highly preorganized tricyclic bis(heteroaryl)-substituted ferrocenyl-imidazo-quinoxaline systems **7** and **8**, in which the redox activity of the ferrocene group is combined with the fluorogenic behavior of the quinoxaline ring[9] and the binding ability of the imidazole ring,[8] embedded into the framework of the imidazo-quinoxaline ring system. Moreover,

Received: May 13, 2015
Published: July 14, 2015

DOI: 10.1021/acs.inorgchem.5b01071
Inorg. Chem. 2015, 54, 7461−7473

the functionalization of the quinoxaline ring with other heterocyclic units, such as furane[12] or thiophene, might also contribute to improve the efficiency of such recognition processes, because of the close proximity of additional binding sites, O or S, to the already existing within the imidazo-quinoxaline framework. The multiresponsive character of these receptors and the ability of the imidazo-quinoxaline ring system to act not only as fluorescent antennae but also as favorable binding sites for cations and anions in the recognition event are most noteworthy.

EXPERIMENTAL SECTION

General and NCIplot analysis were provided in the Supporting Information.

General Procedure for the Preparation of 5-Amino-2,3-disubstituted-6-nitroquinoxalines (3 and 4). To a solution of the appropriate 6-nitro-2,3-disubstituted quinoxaline **1** or **2** (1.63 mmol) and 1,1,1,-trimethylhydrazinium iodide (0.35 g, 176 mmol) in anhydrous DMSO (15 mL) at 50 °C, K^{t}BuO (0.45 g, 3.90 mmol) was added in one portion with stirring. The resulting reaction mixture was stirred overnight, poured over ice and acidified with 10% HCl until pH 3 was achieved. The resulting precipitated was collected by filtration, washed with water, dried and purified by crystallization from CH_2Cl_2 to give the corresponding 5-amino-2,3-disubstituted-6-nitro-quinoxaline **3** or **4**.

*5-Amino-2,3-di(furan-2-yl)-6-nitroquinoxaline (**3**).* Yield: 90% (0.43 g); mp 197−199 °C. ^{1}H NMR (400 MHz, $CDCl_3$) δ 6.55 (dd, J = 1.6 and 3.6 Hz, 1H); 6.59 (dd, J = 2 and 3.6 Hz, 1H); 6.73 (d, J = 3.6 Hz, 1H); 6.81 (d, J = 3.6 Hz, 1H); 7.24 (d, J = 9.6 Hz, 1H); 7.59 (dd, J = 2 and 3.6 Hz, 1H); 7.62 (dd, J = 1.6 and 3.6 Hz, 1H); 8.33 (d, J = 9.6 Hz, 1H). ^{13}C NMR (100 MHz, $CDCl_3$) δ: 112.1, 112.3, 113.2, 114.9; 115.0, 126.7, 127.4, 131.3, 139.9, 143.9, 144.0, 144.3, 145.1, 145.2, 150.2, 150.3. HRMS-ESI: calcd for $C_{16}H_{11}N_4O_4$ $[M+H]^+$, 323.0775. Found: 323.0784.

*5-Amino-2,3-di(thien-2-yl)-6-nitroquinoxaline (**4**).* Yield: 72% (0.41 g); mp 210−212 °C. ^{1}H NMR (400 MHz, $CDCl_3$) δ 7.03 (dd, J = 3.6 and 3.9 Hz,1H); 7.05 (dd, J = 3.6 and 3.9 Hz, 1H); 7.13 (d. J = 9.6, 1H), 7.31 (dd, J = 1.2 and 3.6 Hz, 1H); 7.35 (dd, J = 1.2 and 3.6 Hz, 1H); 7.52 (dd, J = 1.2 and 3.9 Hz, 1H); 7.53 (dd, J = 1.2 and 3.9 Hz, 1H); 8.31 (d, J = 9.6 Hz, 1H). ^{13}C NMR (100 MHz, $CDCl_3$) δ: 114.9, 126.5, 127.4, 127.8, 127.9, 129.4; 129.5; 130.2, 130.4, 131.3, 140.6, 140.7, 143.8, 143.9, 144.2, 149.5. HRMS-ESI: calcd for $C_{16}H_{11}N_4O_2S_2$ $[M+H]^+$, 355.0318. Found: 355.0320.

General Procedure for the Preparation of 5,6-Diamino-2,3-disubstituted Quinoxalines (5 and 6). A solution of the appropriate 5-amino-2,3-disubstituted-6-nitroquinoxaline **3** or **4** (0.62 mmol) in ethanol (5 mL), was heated under reflux temperature. Palladium on charcoal (0.001 g) and hydrazine monohydrate (0.40 mL, 8.25 mmol) then were added stepwise. After the addition of the hydrazine was completed (5 min), another portion of palladium on charcoal (0.002 g) was added, and the resulting mixture was refluxed overnight. Upon cooling, the suspension obtained was filtered over a Celite pad and the solvent evaporated to dryness under reduced pressure. The resulting red solid was then scratched with n-pentane, filtered and crystallized from EtOH−n-hexane (1:1) to give the corresponding diaminoquinoxaline derivative (**5** or **6**).

*5,6-Diamino-2,3-di(furan-2-yl)quinoxaline (**5**).* Yield: 58% (0.10 g); mp 179−181 °C. ^{1}H NMR (400 MHz, $CDCl_3$) δ 4.10 (bs, 4H); 6.50 (dd, J = 0.8 and 3.6 Hz, 1H); 6.52 (dd, J = 2.0 and 3.6 Hz, 1H); 6.56 (dd, J = 1.6 and 3.6 Hz, 1H); 6.67 (dd, J = 0.8 and 3.6 Hz, 1H,); 7.24 (d, J = 8.8 Hz, 1H); 7.54 (d, J = 8.8 Hz, 1H); 7.57 (dd, J = 0.8 and 1.6 Hz, 1H); 7.58 (dd, J = 0.8 and 2.0 Hz 1H). ^{13}C NMR (100 MHz, $CDCl_3$) δ: 111.6, 111.7, 112.0, 127.3, 131.9, 133.4, 136.1, 139.4, 140.4, 143.5, 151.3, 151.7. HRMS-ESI: calcd for $C_{16}H_{13}N_4O_2$ $[M+H]^+$, 293.1033. Found: 293.1034.

*5,6-Diamino-2,3-di(thien-2-yl)quinoxaline (**6**).* Yield: 76% (0.15 g); mp 141−143 °C. ^{1}H NMR (400 MHz, $CDCl_3$) δ 3.99 (bs, 4H); 6.98 (dd, J = 3.6 and 5.2 Hz, 1H); 7.02 (dd, J = 3.6 and 3.9 Hz, 1H); 7.13 (dd, J = 1.2 and 3.6 Hz, 1H); 7.19 (d, J = 8.8 Hz, 1H).7.20 (dd, J = 1.2 and 3.6 Hz, 1H); 7.42 (dd, J = 1.2 and 5.2 Hz, 1H); 7.43 (dd, J = 1.2 and 5.2 Hz, 1H); 7.45 (d, J = 8.8 Hz, 1H). ^{13}C NMR (100 MHz, $CDCl_3$) δ: 119.2, 122.5, 127.1, 127.4, 127.5, 127.8, 128.4, 128.5, 128.8, 132.0, 133.3, 136.0, 141.8, 142.6, 142.9, 144.3. HRMS-ESI: calcd for $C_{16}H_{13}N_4S_2$ $[M+H]^+$, 325.0576. Found: 325.0583.

General Procedure for the Preparation of 2-Ferrocenyl-7,8-disubstituted-3*H*-imidazo[4,5-*f*]quinoxalines (7 and 8). To a solution of the appropriate 5,6-diaminoquinoxalines **5** or **6** (0.70 mmol) in nitrobenzene (15 mL), ferrocenecarboxaldehyde (0.15 g, 0.70 mmol) was added. Then, 0.5 mL of acetic acid was added and the reaction mixture was stirred at 60 °C overnight. Afterward, an aqueous solution of $NaHCO_3$ was added until pH 7 was achieved. The resulting mixture was poured into water (50 mL) and extracted with $CHCl_3$ (2 × 50 mL). The combined organic phases were dried over anhydrous Na_2SO_4, filtered and concentrated under vacuum to give a solid which was purified by column chromatography by using dichloromethane/n-hexane/methanol (9/1/0.5) as an eluent to give **7** or **8** as orange products.

*2-Ferrocenyl-7,8-di(furan-2-yl)-3H-imidazo[4,5-f]quinoxaline (**7**).* Yield: 40% (0.10 g); mp >315 °C (d). ^{1}H NMR (400 MHz, $CDCl_3$) δ 4.13 (s, 5H), 4.46 (st, 2H), 5.03 (st, 2H), 6.50 (dd, J = 3.6 Hz, 1H); 6.54 (dd, J = 1.6 and 3.6 Hz, 1H); 6.57 (dd, J = 2.0 and 3.6 Hz, 1H); 6.70 (d, J = 3.6 Hz, 1H,); 7.60 (dd, J = 0.8 and 2.0 Hz, 1H); 7.61 (dd, J = 0.8 and 1.6 Hz, 1H); 7.93 (d, J = 8.8 Hz, 1H); 8.10 (d, J = 8.8 Hz, 1H); 11.45 (bs, 1H). ^{13}C NMR (100 MHz, $CDCl_3$) δ: 68.2, 70.7, 71.3, 112.8, 113.0, 113.1, 113.8, 124.4, 124.9, 139.3, 141.4, 141.7, 144.7, 145.0, 145.7, 151.7, 151.9, 155.3. HRMS-ESI: calcd for $C_{27}H_{19}FeN_4O_2$ $[M+H]^+$, 487.0858. Found: 487.0861.

*2-Ferrocenyl-7,8-di(thien-2-yl)-3H-imidazo[4,5-f]quinoxaline (**8**).* Yield: 42% (0.15 g); mp >320 °C (d). ^{1}H NMR (400 MHz, $CDCl_3$) δ 4.15 (s, 5H), 4.47 (st, 2H), 5.02 (st, 2H), 7.01 (dd, J = 3.6 and 4.8 Hz, 1H); 7.06 (m, 1H); 7.17 (dd, J = 1.2 and 3.6 Hz, 1H); 7.26 (dd, J = 1.2 and 3.6 Hz, 1H); 7.44 (dd, J = 1.2 and 4.8 Hz, 1H); 7.48 (d, J = 4.8, 1H); 7.89 (d, J = 8.8 Hz, 1H), 8.09 (d, J = 8.8 Hz, 1H), 10.53 (bs, NH). ^{13}C NMR (100 MHz, $CDCl_3$) δ: 67.5, 69.9, 70.4, 73.1, 123.5, 127.5, 127.7, 128.5, 128.8, 129.3, 129.8, 138.7, 141.4, 142.0, 144.7, 144.9, 154.2. HRMS-ESI: calcd for $C_{27}H_{19}FeN_4S_2$ $[M+H]^+$, 519.0401. Found: 519.0401.

Recognition Studies. The recognition properties of compounds **7** and **8** toward a variety of cations (Li^+, Na^+, K^+, Mg^{2+}, Ca^{2+}, Ni^{2+}, Cu^{2+}, Zn^{2+}, Cd^{2+}, Hg^{2+}, and Pb^{2+}), as their perchlorate or triflate salts,[13] and anions (F^-, Cl^-, Br^-, AcO^-, NO_3^-, HSO_4^-, $H_2PO_4^-$, and $HP_2O_7^{3-}$), as tetrabutylammonium salts, was investigated by linear sweep voltammetry (LSV), cyclic voltammetry (CV), and Osteryoung square-wave voltammetry[14] (OSWV), as well as through ultraviolet−visible (UV-vis), fluorescent, and ^{1}H NMR spectroscopic techniques. Titration experiments were further analyzed using the computer program Specfit.[15]

Computational Details. Quantum chemical calculations were performed with the ORCA electronic structure program package.[16] All geometry optimizations were run with tight convergence criteria using the B3LYP[17] functional together with the RIJCOSX algorithm[18] and the Ahlrichs' segmented def2-TZVP basis set.[19] Rational preliminary exploration of the conformational space for the ligands and different host−guest binding modes for the complexes were performed with the lower-quality def2-SVP basis set. In all optimizations and energy evaluations, the latest Grimme's semiempirical atom-pairwise correction (DFT-D3 methods), accounting for the major part of the contribution of dispersion forces to the energy, was included.[20] Solvent effects (acetonitrile) were taken into consideration by using the COSMO solvation model.[21] From these geometries, obtained at the above-mentioned level, all reported electronic data were obtained by means of single-point (SP) calculations using the same functional as well as the more polarized def2-TZVPP basis set. Wiberg bond index (WBI)[22] values were obtained from the natural bond orbital (NBO) population analysis.[23] The topological analysis of the electronic charge density, $\rho(\mathbf{r})$, within Bader's Atoms-In-Molecules (AIM) methodology,[24] was conducted using the AIM2000 software.[25] The computed structures of the complexes were drawn with VMD.[26]

DOI: 10.1021/acs.inorgchem.5b01071
Inorg. Chem. 2015, 54, 7461−7473

RESULTS AND DISCUSSION

Synthesis. The synthesis of the target receptors **7** and **8** was accomplished in 40% and 42% yields, respectively, by a three-step synthetic procedure starting from the readily available 2,3-di(furan-2-yl)-6-nitroquinoxaline (**1**) and 2,3-di(thien-2-yl)-6-nitroquinoxaline[27] (**2**), respectively. (See Scheme 1.) The first step involved an amination reaction through a vicarious nucleophilic substitution of the *ortho* hydrogen atom to the amino group, by using 1,1,1-trimethylhydrazinium iodide in the presence of K^{t}OBu,[28] to give the intermediates **3** (90%) or **4** (72%), which under reduction conditions provided the diamino derivatives **5** (58%) or **6** (76%), required for the construction of the imidazole ring. The structure of these compounds was elucidated using extensive NMR spectral studies (^{1}H NMR, 2D COSY, ^{13}C NMR, and HMQC spectra), as well as high-resolution electrospray ionization mass spectrometry.

Scheme 1. Synthesis of Receptors 7 and 8[a]

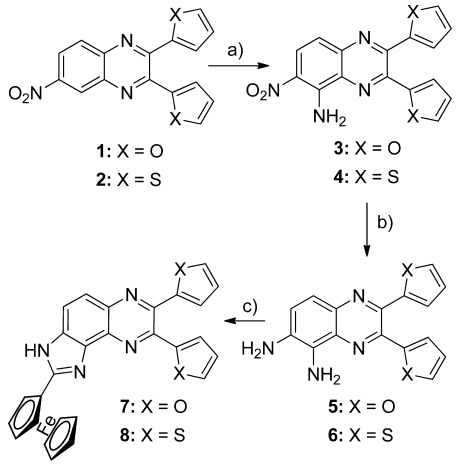

[a]Reagents and conditions: (a) 1,1,1-trimethylhydrazinium iodide, K^{t}BuO, anhydrous DMSO, 50 °C; (b) C/Pd, hydrazine monohydrate, EtOH, Δ; (c) ferrocenecarboxaldehyde, nitrobenzene, AcOH, 60 °C.

Recognition Properties. *Electrochemical Study.* Initial CV studies carried out using electrochemical solutions of **7** and **8** in CH_3CN ($c = 1 \times 10^{-3}$ M) containing 0.1 M [(n-Bu)$_4$N]PF$_6$ as supporting electrolyte, showed that both free receptors exhibited a reversible one-electron ferrocene/ferrocenium redox couple at $E_{1/2}$ = 610 mV and $E_{1/2}$ = 600 mV, respectively, versus the decamethylferrocene (DMFc) redox couple.

The results obtained on stepwise addition of the above-mentioned set of metal cations showed that only addition of Cd^{2+}, Zn^{2+}, Hg^{2+}, and Pb^{2+} metal cations to an electrochemical solution of receptors **7** or **8** induced a remarkable perturbation in their redox potential (see Table S1 and Figures S32−S35 in the Supporting Information). The value of the oxidation potential of the complexes formed is related to the size of the metal cation used, so that the bigger the cation (Hg^{2+}, and Pb^{2+}), the greater oxidation potential observed (Table S1 in the Supporting Information). While Cd^{2+}, Zn^{2+}, Hg^{2+}, and Pb^{2+} metal cations caused the formation of the corresponding metal complexes, addition of Cu^{2+} to receptors either **7** or **8** gave rise to the oxidation of the ferrocene moiety,[29] which was observed through the analysis of the results obtained by LSV (linear sweep voltammetry). These studies showed a significant shift of the sigmoidal voltammetric wave toward cathodic currents when Cu^{2+} were added indicating that this metal cation induced the oxidation of the ferrocene moiety present in the free receptors (Figure S36 in the Supporting Information),whereas the addition of Cd^{2+}, Zn^{2+}, Hg^{2+}, and Pb^{2+} metal cations induced a shift toward more-positive potentials, which is consistent with the complexation process previously observed by CV and OSWV (see Figures S37−S38 in the Supporting Information).[30]

Titration studies with the addition of the above-mentioned set of anions under the same electrochemical condiitons have also been carried out. These studies demonstrated that, although the addition of $H_2PO_4^-$ and AcO^- to both receptors **7** and **8** induced clear electrochemical responses (see Table S1, as well as Figures S39 and S40, in the Supporting Information), the addition of Cl^-, Br^-, NO_3^-, or HSO_4^- anionic species had no effect on their CV and OSWV, even when present in a large excess. Interestingly, the stepwise addition of F^- to both receptors promoted a clear cathodic shift of the corresponding oxidation peaks ($\Delta E_{1/2}$ = −305 mV for **7** and $\Delta E_{1/2}$ = −285 mV for **8**) (Figure S41 in the Supporting Information), as a consequence of the deprotonation of the neutral receptors. This fact was demonstrated both by comparing these results with those obtained from titration with F^- in the presence of acetic acid[31] to prevent the deprotonation of the receptors and those obtained upon titration of the free receptors **7** and **8** with a strong base, such as Bu$_4$NOH, which only induced a deprotonation process.[32] By contrast, the gradual addition of $HP_2O_7^{3-}$ to receptors **7** and **8** promoted the progressive appearance of two new oxidation peaks cathodically shifted by $\Delta E_{1/2}$ = −140 mV and $\Delta E_{1/2}$ = −300 mV in the case of **7** and $\Delta E_{1/2}$ = −180 mV and $\Delta E_{1/2}$ = −290 mV for **8**. However, when the addition of $HP_2O_7^{3-}$ anion to receptors **7** and **8** were performed in the presence of 20 equiv of AcOH only an oxidation peak, cathodically shifted by $\Delta E_{1/2}$ = −85 mV for **7** and $\Delta E_{1/2}$ = −105 mV for **8**, were observed, which clearly indicate that both a deprotonation and a recognition process are simultaneously taking place, while, in the presence of a small amount of acetic acid, only the corresponding hydrogen-bonded adducts are formed (see Table S1 and Figure S43 in the Supporting Information).

These results, taken together, revealed that, although the electrochemical changes observed upon the addition of $H_2PO_4^-$ and AcO^- to both receptors are due to the occurrence of a recognition process with subsequent formation of the corresponding hydrogen-bound adducts, the addition of F^- only leads to a deprotonation process of the neutral receptors and, in the presence of $HP_2O_7^{3-}$ anions, such receptors simultaneously lead to both a recognition process and a deprotonation process.

In summary, the above results revealed that both receptors are capable of electrochemically recognizing metal cations such as Cd^{2+}, Zn^{2+}, Hg^{2+}, and Pb^{2+} and also allow the discrimination of $H_2PO_4^-$ and AcO^- anions from the other anions tested, including HSO_4^-.

After studying the behavior of receptors **7** and **8** toward cations and anions separately, our interest was mainly focused on studying the behavior of both receptor-anion complexes in the presence of metal cations and the receptor−cation complexes in the presence of anions, in order to determine whether these receptors are able to bind simultaneously to a cation and an anion cooperatively or, in other words, if they are able to recognize certain anions in the presence of certain cations bound to them, or *vice versa*. The experimental

DOI: 10.1021/acs.inorgchem.5b01071
Inorg. Chem. 2015, 54, 7461−7473

arrangement used in this study was as follows: in a first step, the corresponding cation-receptor or anion-receptor complexes were preformed in solution and subsequently the electrochemical responses upon addition of suitable counterions were recorded. Furthermore, additional electrochemical experiments, based on the simultaneous addition of the appropriate metal cation and anion to a solution of both receptors, were also carried out.

From the series of experiments carried out, we found four different situations that clearly demonstrate the effective capability of receptors **7** and **8** to act as appropriate hosts in ion-pair recognition processes. First of all, we determine the affinities of metal cations such as Cd^{2+}, Pb^{2+}, Zn^{2+}, and Hg^{2+}, which individually had demonstrated their ability to form cationic complexes with receptors **7** and **8**, toward the preformed $[\mathbf{R}{\cdot}H_2PO_4]^-$ complex ($E_{1/2}$ = 470 mV for **R** = **7** and $E_{1/2}$ = 440 mV for **R** = **8**). In these cases, new oxidation peaks appeared at $E_{1/2}$ values higher than that observed upon complexation with those metal cations alone (see Table 1 and Figures 1a and 1b, as well as Figures S44−S47 in the Supporting Information).

Table 1. Electrochemical Data of the Ion-Pair Complexes Formed by Receptors 7 and 8 in the Presence of Several Cations and Anions

ion-pair complexes	$E_{1/2}$	$\Delta E_{1/2}$[a]
7 + Cd^{2+} + $H_2PO_4^-$	875	265
7 + Pb^{2+} + $H_2PO_4^-$	875	265
7 + Hg^{2+} + $H_2PO_4^-$	835	225
7 + Zn^{2+} + $H_2PO_4^-$	855	245
7 + Ni^{2+} + $H_2PO_4^-$	870	255
7 + Mg^{2+} + $H_2PO_4^-$	860	250
8 + Cd^{2+} + $H_2PO_4^-$	865	265
8 + Pb^{2+} + $H_2PO_4^-$	865	265
8 + Hg^{2+} + $H_2PO_4^-$	850	250
8 + Zn^{2+} + $H_2PO_4^-$	860	260
8 + Ni^{2+} + $H_2PO_4^-$	865	265
8 + Mg^{2+} + $H_2PO_4^-$	855	255
7 + Cd^{2+} + HSO_4^-	870	260
7 + Pb^{2+} + HSO_4^-	855	245
7 + Hg^{2+} + HSO_4^-	830	220
7 + Zn^{2+} + HSO_4^-	830	220
7 + Ni^{2+} + HSO_4^-	850	240
7 + Mg^{2+} + HSO_4^-	870	260
8 + Cd^{2+} + HSO_4^-	865	265
8 + Pb^{2+} + HSO_4^-	875	275
8 + Hg^{2+} + HSO_4^-	835	235
8 + Zn^{2+} + HSO_4^-	855	255
8 + Ni^{2+} + HSO_4^-	860	260
8 + Mg^{2+} + HSO_4^-	870	270

[a] $\Delta E_{1/2} = E_{1/2\ \text{complex}} - E_{1/2\ \text{free receptor}}$, mV vs DMFc; error = ±0.002 V.

Moreover, the addition of Ni^{2+} and Mg^{2+} cations, which, in turn, cannot bind to the free receptors, to electrochemical solutions of $[\mathbf{R}{\cdot}H_2PO_4]^-$ complexes (**R** = **7** and **8**), induced the appearance of new oxidation peaks at $E_{1/2}$ values whose magnitudes are comparable (see Table 1 and Figures 1c and 1d, as well as Figures S48 and S49 in the Supporting Information) to those observed when Cd^{2+}, Pb^{2+}, Zn^{2+}, and Hg^{2+} metal cations were added. These findings illustrate a rare case of metal cation recognition (Ni^{2+}, and Mg^{2+}) by receptors **7** and **8**, which appear to display absolutely no affinity for these metal

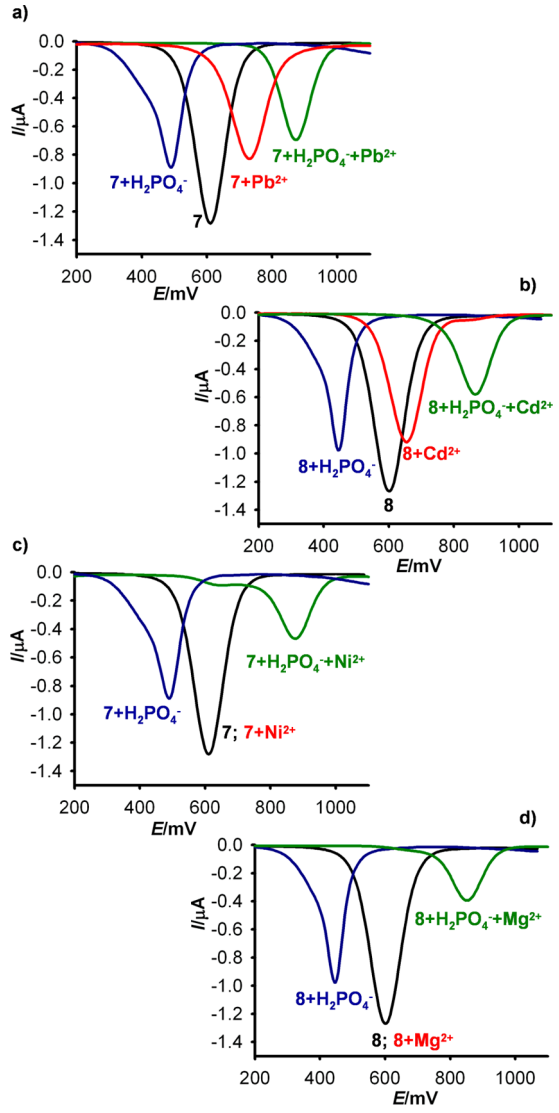

Figure 1. Evolution of the OSWV of receptors **7** and **8** in CH_3CN (c = 1 × 10^{-3} M) in the presence of $[(n\text{-Bu})_4N]PF_6$ as supporting electrolyte, versus decamethylferrocene (DMFc) redox couple, scanned at 0.1 V s^{-1}, (black lines), in the presence of $H_2PO_4^-$ (blue lines) and the indicated metal cations (red lines) and after the initial addition of $H_2PO_4^-$, followed by the addition of the appropriate metal cation (green lines).

cations in the absence of a suitable anionic guest, but which binds very strongly in the presence of co-bound anionic species ($H_2PO_4^-$).

Furthermore, a similar effect was also found when Cd^{2+}, Pb^{2+}, Zn^{2+}, and Hg^{2+} metal cations were added to an electrochemical solution of receptors **7** and **8** in the presence of HSO_4^- anion $[\mathbf{R}{\cdot}HSO_4]^-$, which did not effect on the $E_{1/2}$ of the free receptors. In these cases, new oxidation peaks also appeared at $E_{1/2}$ values higher than that observed upon complexation of the free receptors with those metal cations alone (see Table 1 and Figures 2a and 2b, as well as Figures S50−S53 in the Supporting Information).

However, as previously mentioned, the most interesting case was that observed by adding a metal cation (Ni^{2+} and Mg^{2+}) that did not interact with the free receptors **7** and **8**, to an electrochemical solution of these receptors containing an anion (HSO_4^-) which either interacted with them. The results

DOI: 10.1021/acs.inorgchem.5b01071
Inorg. Chem. 2015, 54, 7461−7473

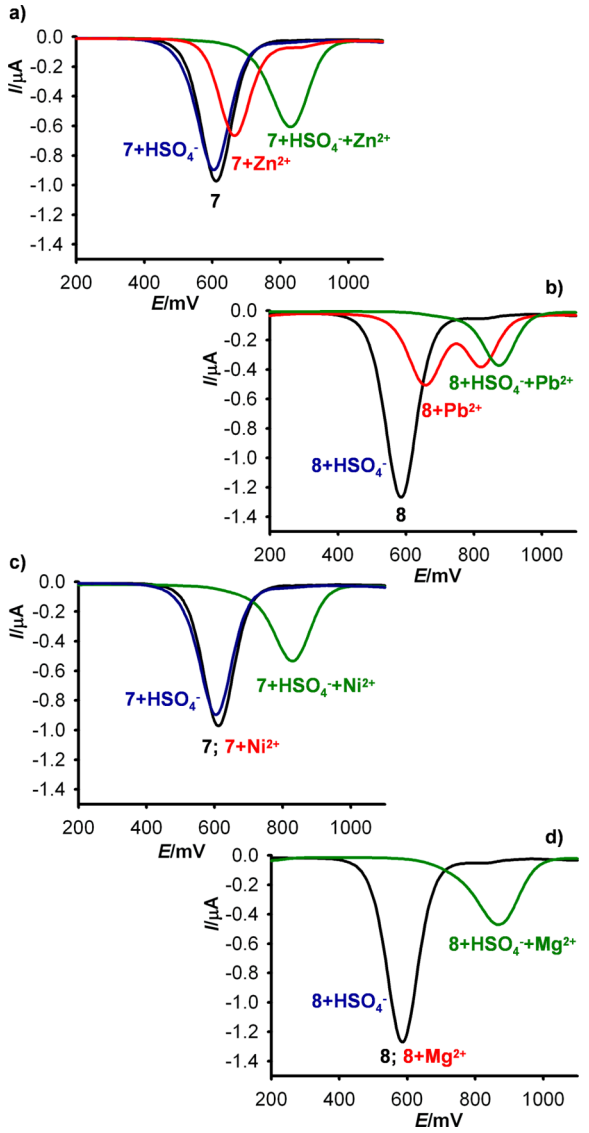

Figure 2. Evolution of the OSWV of receptors **7** and **8** in CH_3CN (c = 1 × 10^{-3} M) in the presence of $[(n\text{-Bu})_4N]PF_6$ as the supporting electrolyte, versus decamethylferrocene (DMFc) redox couple, scanned at 0.1 V s^{-1}, (black lines), in the presence of HSO_4^- (blue lines) and the indicated metal cations (red lines) and after the initial addition of HSO_4^-, followed by the addition of the appropriate metal cation (green lines).

obtained clearly evidenced the existence of oxidation peaks at the $E_{1/2}$ values showed in Table 1 (Figures 2c and 2d, as well as Figures S54 and S55 in the Supporting Information). This effect should be a result of the simultaneous participation of the cation and anion in a favorable disposition to be recognized by the receptors, which represents a novel type of heteroditopic receptor that displays no affinity for "free" ions but does exhibit enhanced binding of ion pairs.[33]

Previous studies have shown that, because of the opposite nature of the electrostatic interactions between the ferrocenium moiety and the complexed cation and anion, the overall potential shift of a ferrocene receptor upon complexation with an ion-pair is smaller than complexing the individual ions.[8k,30a] By contrast, the electrochemical data resulting from the ion-pair recognition by **7** and **8** shown anodic shifts of the corresponding oxidation peaks, which are higher than that resulting from the complexation with the metal cations alone. This fact pointed to an unusual nonadditive mechanism mainly affecting the ferrocene unit, suggesting that a contact arrangement between those ion pairs and the receptors **7** and **8** must be the favorable binding modes (see the Theoretical Calculations section below).

Absorption and Emission Study. The binding properties of receptors **7** and **8** toward metal cations and anions were also examined by using absorption and emission techniques. The UV-vis absorption spectrum of receptors **7** and **8** in CH_3CN (c = 10^{-5} M) exhibit two absorptions bands, centered at ∼280 and 325 nm. (See Table 2, as well as Figures S56 and S57 in the Supporting Information). The spectrophotometric results obtained upon the progressive addition of the metal cations tested clearly show that receptor **7** selectively recognizes Zn^{2+} and Pb^{2+} metal cations through this optical channel, whereas receptor **8** recognizes Hg^{2+} and Pb^{2+} cations in the same way. In the cases of both **7** and **8**, the presence of well-defined isosbestic points observed during the titration processes (see Table 2, as well as Table S2 in the Supporting Information) suggested the existence of a two-state equilibrium, which means there is only one spectrally distinct stable complex in solution.

Table 2. UV-vis Data of Receptors 7 and 8 in the Presence of Selected Cations, Anions, and Ion Pairs

receptor	cation added	ion pair	λ (× 10^{-4} nm), ε (M^{-1} cm^{-1})	isosbestic points
7			280 (0.260), 325 (0.405)	
7	Zn^{2+}		272 (0.244), 322 (0.368), 380 (sh)	270, 350
7	Ni^{2+}			
7		$H_2PO_4^-$ + Zn^{2+}	260 (0.243), 287 (0.257), 345 (0.338)	370, 340, 425
7		HSO_4^- + Ni^{2+}	270 (0.253), 323 (0.397), 380 (0.140)	
8			285 (0.256), 325 (0.370)	
8	Pb^{2+}		270 (0.232), 325 (0.328), 385 (sh)	270, 365
8	Mg^{2+}			
8		HSO_4^- + Pb^{2+}	264 (0.287), 325 (0.326), 380 (0.194), 480 (0.020)	275, 425, 460
8		$H_2PO_4^-$ + Mg^{2+}	264 (0.281), 325 (0.346), 380 (0.171), 480 (0.026)	275, 425, 460

Interestingly, unlike that observed in the electrochemical titrations with cations, no spectrophotometric changes were detected upon addition of any anion tested, suggesting that the anion recognition process was not significant at the lower concentrations used in this technique.

Having established binding abilities of **7** and **8** toward cations and anions, we next focused our attention to the study of the effect that the cation or anion binding could have on the counterion recognition (in other words, the ability of these compounds to act as ion-pair recognition receptors).

As it has been already mentioned, addition of HSO_4^- and $H_2PO_4^-$ anions did not cause any perturbation on the UV-vis spectrum of the free receptors **7** and **8**. However, when they were added to solutions of the previously formed $[7{\cdot}Zn]^{2+}$, $[7{\cdot}Pb]^{2+}$, $[8{\cdot}Pb]^{2+}$, or $[8{\cdot}Hg]^{2+}$ cationic complexes, slight perturbations of the UV-vis of the free receptors were observed, although the magnitude of such changes were not enough for an accurate calculations of the association constants. Furthermore, the same results were obtained when the

DOI: 10.1021/acs.inorgchem.5b01071
Inorg. Chem. 2015, 54, 7461−7473

experiments were performed inversely: addition of the metal cation to a solution of the preformed anionic complexes of receptors **7** and **8** with the corresponding anion (see Figure 3, as well as Figures S60 and S61 in the Supporting Information).

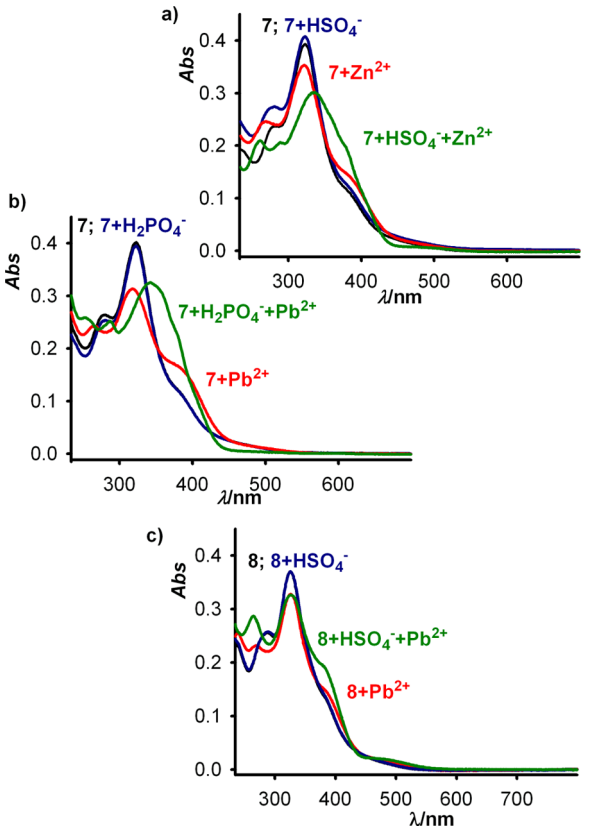

Figure 3. Evolution of the UV-vis spectra of **7** (top) and **8** (bottom) upon addition of the indicated metal cations to a solution of the free receptors in CH_3CN ($c = 1 \times 10^{-5}$ M), containing the appropriate anion.

Moreover, to test if the binding ability of cations or anions by these receptors was influenced by the existence of appropriate counterions in their solutions, we conducted a second set of UV-vis experiments based on the addition of metal cations, which did not promote any change in the absorption spectra of the free receptors (Cd^{2+}, Ni^{2+}, and Mg^{2+} in the case of **7** and Cd^{2+}, Ni^{2+}, Zn^{2+}, and Mg^{2+} in the case of **8**) to solutions of these receptors containing HSO_4^- and $H_2PO_4^-$ anions. From the analysis of the spectra obtained is clear that, in some cases, the cation binding can only be detected in the presence of these anions, demonstrating that **7** and **8** bind the ion pair where no affinity for either of the discrete ions was observed: in other words, they display the rare property consistent with the cooperative AND recognition of ion pairs. Figure 4, as well as Figures S62−S64 in the Supporting Information, illustrate this ion-pair binding behavior of both receptors and the cases for which such cooperative binding effect was not observed.

Assessment of the affinity of the ions also came from observing the extent to which the fluorescence intensity of receptors **7** and **8** was affected in the presence of the above-mentioned set of anions and cations. As expected, receptors **7** and **8** showed a very weak fluorescence in CH_3CN ($c = 2 \times 10^{-6}$ M for **7** and 1×10^{-5} M for **8**) revealing that $\lambda_{exc} = 345$ nm is an ideal excitation wavelength for the case of **7** and $\lambda_{exc} =$

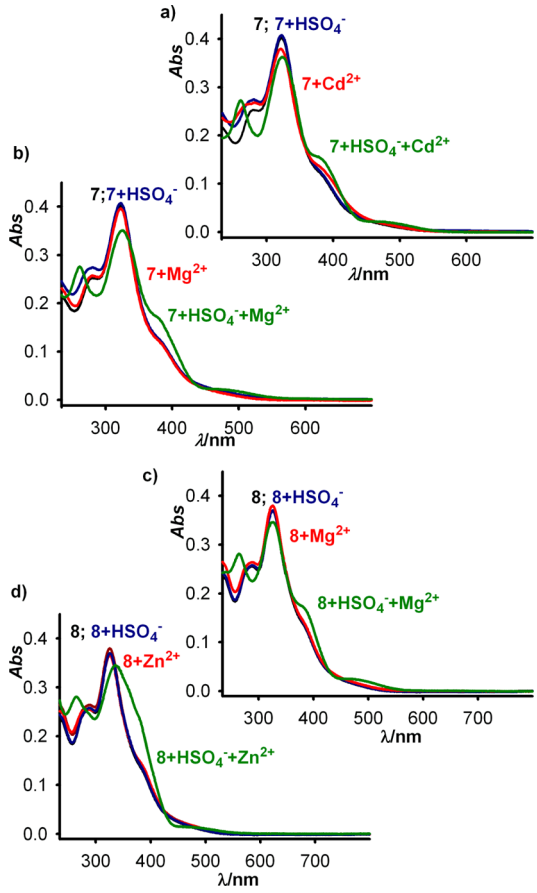

Figure 4. Evolution of the UV-vis of **7** (up) and **8** (bottom) upon addition of the indicated metal cations to a solution of the free receptors in CH_3CN ($c = 1 \times 10^{-5}$ M), containing the appropriate anion.

340 nm for **8**. In each case, the corresponding emission spectrum displayed a very weak band with rather low quantum yields $\lambda = 475$ nm ($\Phi = 2.7 \times 10^{-4}$) for **7** and $\lambda = 465$ nm ($\Phi = 4 \times 10^{-4}$) for **8**.

The binding behavior of **7** and **8** toward metal cations monitored through fluorescence titration experiments demonstrated that, in the case of **7**, only Pb^{2+} and Zn^{2+} cations promoted a remarkable increase of the emission band at 475 nm, while such changes were more slight when Cd^{2+}, Pb^{2+}, and Zn^{2+} cations were added to receptor **8** (see Table S3 and Figures S65−S67 in the Supporting Information). From the titration data, the corresponding association constants[15] and detection limits[34] were calculated (see Table S3 and Figures S68 and S69 in the Supporting Information). Interestingly, these fluorescent titration studies clearly shown that receptor **7** is able to discriminate Cd^{2+} from Zn^{2+}, through a fluorescent channel, which constitutes a challenge to be considered in the field of receptor design, because of the fact that Cd^{2+} cations causes toxicity in living cells, disrupting the transport of the essential Zn^{2+} into and out of cells.[35]

Moreover, the affinity of **7** and **8** toward the set of anions above-mentioned was also tested by emission spectroscopy, although the interactions of these anions with both receptors were negligible.

To verify that receptors **7** and **8** can be used for ion-pair recognition, the simultaneous complexation of appropriate metal cations and anions was also investigated by fluorescence

DOI: 10.1021/acs.inorgchem.5b01071
Inorg. Chem. 2015, 54, 7461−7473

spectroscopy. In a first set of experiments, $Zn^{2+}$and Pb^{2+} cations were chosen as the cationic partners, since it was demonstrated that both displayed a high affinity for receptors **7** and **8**. Thus, the addition of 1 equiv HSO_4^- to a solution containing the preformed $[7{\cdot}Pb]^{2+}$ cationic complex results in a dramatic enhancement of the emission band at 475 nm (chelation-enhanced fluorescence (CHEF) = 640), and the quantum yield ($\Phi = 2.84 \times 10^{-1}$) resulted in a 5-fold increase. Similar behavior was observed upon addition of this anion to the complex $[7{\cdot}Zn]^{2+}$ complex, which induced an enhancement of the emission band (CHEF = 565), and a 7-fold increase in the quantum yield ($\Phi = 1.58 \times 10^{-1}$) (see Figure 5a and Table 3).

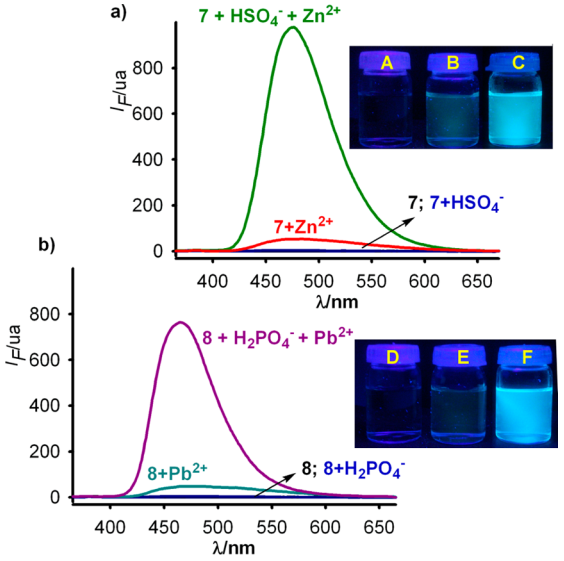

Figure 5. Evolution of the emission spectra of (a) **7** ($c = 2 \times 10^{-6}$ M) and (b) **8** ($c = 10^{-5}$ M) upon addition of the indicated anions to a solution containing the appropriate $[7{\cdot}Zn]^{2+}$ or $[8{\cdot}Pb]^{2+}$ complex. Inset in each panel shows visual changes observed upon the titration processes. (In panel a, A = **7**, B = $[7{\cdot}Zn^{2+}]$, and C = $[7{\cdot}HSO_4^-{\cdot}Zn^{2+}]$; in panel b, D = **8**, E = $[8{\cdot}Pb^{2+}]$, and F = $[8{\cdot}H_2PO_4^-{\cdot}Pb^{2+}]$.)

Note that similar interactions of the complexes $[8{\cdot}Pb]^{2+}$ and $[8{\cdot}Zn]^{2+}$ with $H_2PO_4^-$ were also observed (see Figure 5b and Table 3). Moreover, in both cases, identical results were obtained either by changing the addition sequence or when the addition of anion and cation was carried out simultaneously. These findings demonstrate that receptors **7** and **8** display a dramatic enhancement of HSO_4^- or $H_2PO_4^-$ anion binding, respectively, by co-bound Zn^{2+} or Pb^{2+} cations, whereas no affinity of the free receptors by HSO_4^- or $H_2PO_4^-$ anions were detected (see Figures S70 and S71 in the Supporting Information).

In a second set of experiments, we tested the ability of **7** and **8** to coordinate and sense a cation and an anion at the same time, but using cations and anions that did not show any affinity for those receptors. Thus, titration experiments were performed via the addition of Mg^{2+}, Cd^{2+}, or Ni^{2+} to a solution of **7**, or Mg^{2+}, and Ni^{2+} to a solution of **8**, both containing the HSO_4^- or $H_2PO_4^-$ anions. Interestingly, in all the cases, the addition of the metal cations was accompanied by an increase in emission intensity, although the magnitude of such an increase is strongly dependent on the cation and anion under study (see Figure 6 and Table 3, as well as Figures S73 and S74 in the Supporting Information).

Table 3. Emission Data of Receptors 7 and 8 in the Presence of Ion Pairs

receptor	ion pair	λ_{em} (nm)	Φ (CHEF)[a]
7		475	2.7×10^{-4}
7	$H_2PO_4^-$ + Cd^{2+}	480	0.140 (400)
7	$H_2PO_4^-$ + Zn^{2+}	475	0.247 (940)
7	$H_2PO_4^-$ + Pb^{2+}	475	0.249 (965)
7	$H_2PO_4^-$ + Ni^{2+}	485	0.080 (230)
7	$H_2PO_4^-$ + Mg^{2+}	480	0.188 (420)
7	HSO_4^- + Cd^{2+}	475	0.144 (470)
7	HSO_4^- + Zn^{2+}	475	0.158 (565)
7	HSO_4^- + Pb^{2+}	475	0.284 (640)
7	HSO_4^- + Ni^{2+}	470	0.047 (95)
7	HSO_4^- + Mg^{2+}	470	0.106 (360)
8	$H_2PO_4^-$ + Cd^{2+}	465	0.058 (508)
8	$H_2PO_4^-$ + Zn^{2+}	465	0.053 (433)
8	$H_2PO_4^-$ + Pb^{2+}	465	0.056 (477)
8	$H_2PO_4^-$ + Mg^{2+}	465	0.051 (372)
8	$H_2PO_4^-$ + Ni^{2+}	465	0.036 (229)
8	HSO_4^- + Cd^{2+}	465	0.058 (392)
8	HSO_4^- + Zn^{2+}	465	0.053 (462)
8	HSO_4^- + Pb^{2+}	465	0.056 (350)
8	HSO_4^- + Mg^{2+}	465	0.051 (253)
8	HSO_4^- + Ni^{2+}	465	0.036 (172)

[a]CHEF = chelation-enhanced fluorescence.

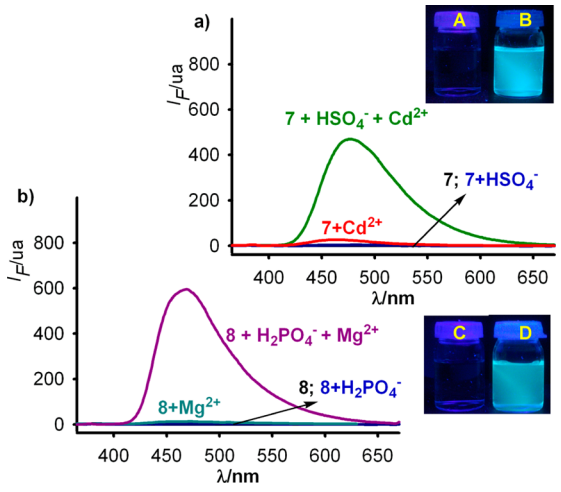

Figure 6. Evolution of the emission spectra of (a) **7** ($c = 2 \times 10^{-6}$ M) and (b) **8** ($c = 10^{-5}$ M), upon addition of the indicated anions to a solution containing the appropriate (Cd^{2+} or Mg^{2+}) metal cation. Inset in each panel shows visual changes observed upon the titration processes. (In panel a, A = **7** and B = $[7{\cdot}HSO_4^-{\cdot}Cd^{2+}]$; in panel b, C = **8** and D = $[8{\cdot}H_2PO_4^-{\cdot}Mg^{2+}]$.

Altogether, the results obtained, once again, demonstrate that **7** and **8** behave as ion-pair receptors, with binding of the metal cations probably being a prerequisite for the recognition of the anion into the cavity formed by the ferrocene unit and the heterocyclic ring. This positive cooperativity should then be due to the fact that these two ions can be bound to the receptors as a contact ion pair.

The stoichiometries and association constants of the ion-pair complexes formed were determined by the changes in the emission responses of the preformed cation−receptor complexes upon the addition of aliquots of the appropriate anion,

DOI: 10.1021/acs.inorgchem.5b01071
Inorg. Chem. 2015, 54, 7461−7473

and these are summarized in Table S4 in the Supporting Information. Moreover, the stoichiometries proposed from the spectroscopic data have been further confirmed by ESI-MS (see Figures S78−S90 in the Supporting Information).

For the reported constants to be taken with confidence, we have proved the reversibility of the ion-pair formation. If the process is reversible, depletion of the ions that coordinate the receptors must produce a change of either in the CV, or in the absorption, emission, or ^{1}H NMR spectrum, causing it to revert to the original spectrum. In this context, we have carried out the following experimental test. First, the CV, UV-vis, emission, and ^{1}H NMR spectra of the ion-pair complexes with receptor **7** in CH_2Cl_2 were recorded and then to the solutions of such complexes aliquots of water were added. The resulting solutions were stirred for 15 min and the corresponding organic layer was separated and dried. The CV, and the corresponding optical or ^{1}H NMR spectra, were then recorded and found to be the same as those of free receptor **7**. Afterward, appropriate amounts of the ions were added to this solution, and the initial CV, UV-vis, emission and ^{1}H NMR spectra of the ion-pair complexes derived from **7** were fully recovered. These experiments were carried out over several cycles, and the corresponding CV and spectra were recorded after each step, thus demonstrating the high degree of reversibility of the complexation/decomplexation process (see Figure S91 in the Supporting Information). Similar studies were carried out using receptor **8** and the adequate ions, which confirm the reversibility of this process between this receptor and such ionic species (see Figure S92 in the Supporting Information).

^{1}H NMR Study. An additional proof about the influence that the binding of a charged guest by receptor **7** or **8** can exert on the subsequent coordination of the pairing ion is provided by the shifts observed in their ^{1}H NMR spectra, carried out in CD_3CN solutions, upon gradual addition of the appropriate guest: a divalent metal cation or an anion. To investigate those interactions, the following experiments were carried out: (i) titrations with cations (Zn^{2+}, Cd^{2+}, and Pb^{2+}) and anions ($H_2PO_4^-$) which have individually demonstrated ability to coordinate with those receptors; (ii) titrations with cations capable of coordinating with the receptors (Zn^{2+}, Cd^{2+}, and Pb^{2+}) but in the presence of HSO_4^- anion, which did not show such ability; and (iii) titrations in the presence of cations (Mg^{2+} and Ni^{2+}), and anions (HSO_4^-) that showed no affinity for these receptors. In all cases, the most characteristic and general changes observed in the ^{1}H NMR of **7** and **8**, during the gradual addition of these ionic guests, are illustrated in Figure 7, as well as Figures S93−S117 and Tables S5−S8 in the Supporting Information. As shown in these figures, the most relevant chemical shift changes upon the addition of metal cations, such as Zn^{2+}, Cd^{2+}, and Pb^{2+}, were those related to the Hα and Hβ protons within the monosubstituted Cp ring of the ferrocene moiety, which are significantly upshielded. Thus, the spectra recorded for [**7**·M^{2+}] (M = Zn, Cd, and Pb) exhibited similar patterns for ferrocene protons as those recorded for [**8**·M^{2+}] (M = Zn, Cd, and Pb). However, by adding $H_2PO_4^-$ or HSO_4^- anions to these preformed [**7**·M^{2+}] and [**8**·M^{2+}] complexes, the ferrocenyl protons were significantly moved downfield, which strongly supports the interaction of the anion, to a certain extent, with the ferrocene moiety of the metal complexes initially formed (see the Theoretical Calculations section below). Moreover, protons within the fused imidazoquinoxaline core and those of the furane or thiophene rings are progressively shifted downfield as aliquots of the corresponding anion were added to the solution containing the cation−receptor complexes, which also indicate the change in the chemical environment of the imidazoquinoxaline cavity, as the ion-pair complex formation is taking place.

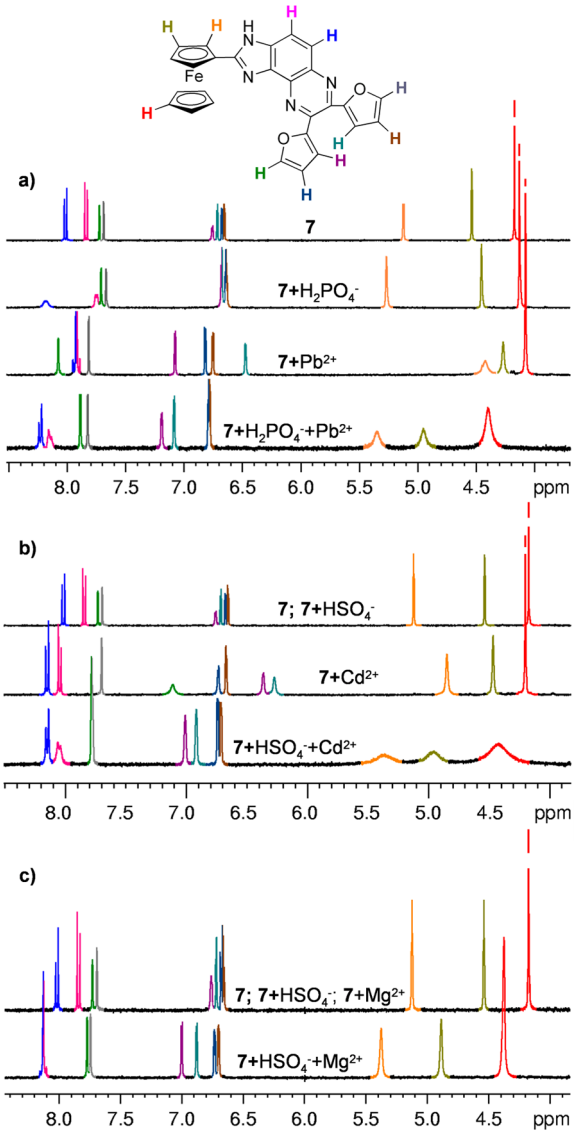

Figure 7. Evolution of the ^{1}H NMR of **7** (CD_3CN) in the presence of the indicated species.

Theoretical Calculations. Quantum chemical calculations were undertaken in order to unveil the structural and electronic signature controlling the aforementioned responses toward anions and cations and, especially, the enhanced heteroditopic behavior of the receptors toward ion pairs, in cases where no affinity was observed for the isolated ionic constituents. Receptors **7** and **8** showed a preference for the tautomeric form bearing the imidazole H atom on N(1), by 0.43 and 0.49 kcal/mol, with respect to the other isomers $\mathbf{7}^{N(3)H}$ and $\mathbf{8}^{N(3)H}$, respectively. Next, the behavior of **7** toward the dihydrogen phosphate anion, as well as Zn^{2+} and Pb^{2+} cations (as triflate and perchlorate, respectively), was studied. The reaction with the anion is expected to lead to a $[\mathbf{7}\cdot H_2PO_4]^-$ species featuring two main hydrogen bond (HB) anchoring interactions involving the imidazole N(1)−H and one of the anion P═O groups ($\angle$NHO = 176.2°; $d_{NH\cdots O}$ = 1.682 Å; WBI = 0.086; $\rho(r)$ = 4.93 × 10^{-2} e/a_0^3) and a P−OH group as HB donor toward

DOI: 10.1021/acs.inorgchem.5b01071
Inorg. Chem. 2015, 54, 7461−7473

the quinoxaline N(9) acceptor site (∠NHO = 171.2°; $d_{N\cdots HO}$ = 1.826 Å; WBI = 0.073; $\rho(r)$ = 4.07 × 10^{-2} e/a_0^3) (see Figure 8a). Three other secondary CH···O HBs involving Cp and furyl CH units are also observed.

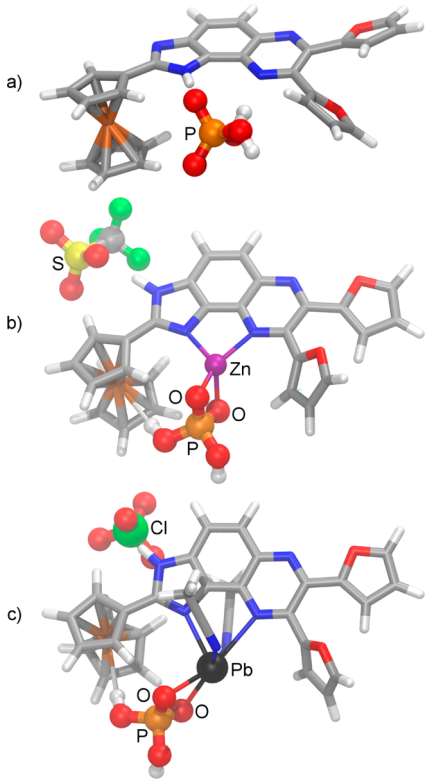

Figure 8. Computed ($COSMO_{MeCN}$/B3LYP-D3/def2-TZVP) most stable geometries for complexes (a) $[7\cdot(H_2PO_4)]^-$, (b) $[7\cdot Zn(H_2PO_4)]^+OTf^-$, and (c) $[7\cdot Pb(H_2PO_4)(MeCN)_2]^+ClO_4^-$. Receptors are displayed in capped sticks, and guest molecules are depicted in ball-and-stick representations.

In terms of its electrochemical properties, the most relevant signature of this anionic unit $[7\cdot H_2PO_4]^-$ is the energy of its highest occupied molecular orbital (HOMO), basically located at the ferrocene group, which is significantly higher than the free receptor (Table 4), as expected for an increased electron density at the electroactive center. This agrees with the observed cathodic shift of the redox signal (Figure 1).

In silico reactions of receptor **7** with $Zn(OTf)_2$ and $Pb(ClO_4)_2$ afford complexes that should be represented as $[7\cdot Zn(OTf)]^+OTf^-$ and $[7\cdot Pb(ClO_4)(MeCN)_2]^+ClO_4^-$, respectively (see the Supporting Information). Both complexes are better described as *ligand-separated ion pairs*, because the metal cation, together with one anionic ligand (i.e., M^{2+} and A^-, forming a $[M-A]^+$ monocation), is chelated by imidazole N(1) and quinoxaline N(9) donor atoms at the concave side of the receptor, whereas the second anionic unit acts as HB acceptor and binds to the imidazole N(3)−H group at the convex side (*vide infra*). In the case of the Pb^{2+} salt, the coordination sphere around the large metal cation is further saturated with two CH_3CN solvent molecules. As expected, the electrochemically relevant consequence of complexation is the reduction in the HOMO energy (see Table 4), because of the decrease of electron density at electroactive Fe atom, in agreement with the observed anodic shift of the redox signal (see Table S1 in the Supporting Information). When HSO_4^- or $H_2PO_4^-$ anions are

Table 4. HOMO Energies and Composition in Computed Species

	ε (eV)	$\Delta\varepsilon^a$ (eV)	%Fe[b]
7	−5.524		62.6
$[7\cdot H_2PO_4]^-$	−5.303	+0.221	65.1
$[7\cdot Zn(OTf)]^+OTf^-$	−5.765	−0.241	77.0
$[7\cdot Zn(H_2PO_4)]^+OTf^-$	−5.930	−0.406	69.9
$[7\cdot Pb(ClO_4)(MeCN)_2]^+ClO_4^-$	−5.683	−0.159	78.4
$[7\cdot Pb(H_2PO_4)(MeCN)_2]^+ClO_4^-$	−5.837	−0.313	71.1
8	−5.354		58.7
$[8\cdot HSO_4]^-$	−5.323	+0.031	66.4
$[8\cdot Mg(ClO_4)]^+ClO_4^-$	−5.722	−0.368	75.3
$[8\cdot Mg(HSO_4)]^+ClO_4^-$	−5.931	−0.577	66.4
$[8\cdot Mg(HSO_4)]^+HSO_4^-$	−5.885	−0.531	67.8
$[8\cdot Mg(HSO_4)(H_2O)]^+HSO_4^-$	−5.849	−0.495	66.4

[a]Relative to the free ligand. [b]Contribution of Fe, according to the Löwdin reduced-orbital population.

added to the above-mentioned complexes, a critical step occurs upon the addition of the first equivalent as the metal-bound anionic ligand at the concave side is preferentially exchanged. Thus, in the case of dihydrogen phosphate, complexes $[7\cdot Zn(H_2PO_4)]^+OTf^-$ and $[7\cdot Pb(H_2PO_4)(MeCN)_2]^+ClO_4^-$ are formed in the first step as the most stable products (see Figure 8).[36] In both cases, the most salient common feature is the enhanced acidity of the metal-bound $H_2PO_4^-$ ligand in close spatial proximity to the ferrocene substituent. This enables protonation at the Fe center and causes an additional decrease of the HOMO energy (Table 4), thus giving support to the observed enhanced anodic shift of the redox signal (Table 1). Complex $[7\cdot Zn(H_2PO_4)]^+OTf^-$ displays a triflate anion bound through a typical NH···O moderately strong HB (∠NHO = 167.1°; $d_{NH\cdots O}$ = 1.875 Å; WBI = 0.046; $\rho(r)$ = 3.14 × 10^{-2} e/a_0^3) and two weak HBs with Cp H atoms ($d_{CH\cdots O}$ = 2.204 and 2.605 Å; WBI = 0.011 and 0.002; $\rho(r)$ = 1.54 × 10^{-2} e/a_0^3, no bond critical point (BCP) found for the second interaction). The Zn^{2+} ion lies in a distorted tetrahedral environment with two N coordinating atoms ($d_{Zn\cdots N}$ = 2.026 and 2.075 Å; WBI = 0.141 and 0.142; $\rho(r)$ = 8.08 × 10^{-2} and 7.46 × 10^{-2} e/a_0^3) and two bonds to O atoms ($d_{Zn\cdots O}$ = 2.037 and 2.065 Å; WBI = 0.123 and 0.095; $\rho(r)$ = 7.23 × 10^{-2} and 6.76 × 10^{-2} e/a_0^3). These two O atoms form additional HBs with CH groups located at Cp ($d_{CH\cdots O}$ = 2.353 and 2.448 Å; WBI = 0.005 and 0.006; $\rho(r)$ = 1.03 × 10^{-2} and 1.18 × 10^{-2} e/a_0^3) or furyl rings ($d_{CH\cdots O}$ = 2.472 Å; WBI = 0.004; $\rho(r)$ = 0.98 × 10^{-2} e/a_0^3). The Fe···H interaction very much resembles a typical moderately strong HB (∠OHFe = 177.2°; $d_{OH\cdots Fe}$ = 2.754 Å; WBI = 0.003; $\rho(r)$ = 1.12 × 10^{-2} e/a_0^3).

In the case of the $[7\cdot Pb(H_2PO_4)(MeCN)_2]^+ClO_4^-$ complex, the metal cation is located in a hemidirected[37] coordination geometry, because of the effect of the stereochemically active electron lone pair, typical of Pb(II) centers.[38] As a result, the metal environment consists of a distorted pentagonal pyramid comprised of two receptor N atoms ($d_{Pb\cdots N}$ = 2.598 and 2.876 Å; WBI = 0.190 and 0.091; $\rho(r)$ = 4.01 × 10^{-2} and 2.44 × 10^{-2} e/a_0^3) at the strong apical position and one equatorial position, two dihydrogen phosphate O atoms ($d_{Pb\cdots O}$ = 2.554 and 2.556 Å; WBI = 0.131 and 0.120; $\rho(r)$ = 3.98 × 10^{-2} and 3.95 × 10^{-2} e/a_o^3) and two additional acetonitrile N atoms ($d_{Pb\cdots N}$ = 2.715 and 2.760 Å; WBI = 0.114 and 0.113; ρ(r) = 2.84 × 10^{-2} and 2.61 × 10^{-2} e/a_o^3) at both sides of the receptor main plane. The

DOI: 10.1021/acs.inorgchem.5b01071
Inorg. Chem. 2015, 54, 7461−7473

combination of enhanced OH acidity and spatial proximity enables effective iron protonation by the coordinating $H_2PO_4^-$ ligand (∠OHFe = 170.8°; $d_{OH\cdots Fe}$ = 2.662 Å; WBI = 0.008; $\rho(r)$ = 1.25 × 10^{-2} e/a_0^3). The perchlorate anion at the receptor convex side is anchored by a main HB of N−H···O type (∠NHO = 151.7°; $d_{NH\cdots O}$ = 1.876 Å; WBI = 0.039; $\rho(r)$ = 3.06 × 10^{-2} e/a_0^3) and four other weaker HBs with Cp H atoms ($d_{CH\cdots O}$ = 2.505, 2.565, and 2.612 Å; WBI = 0.004, 0.003, and 0.001; $\rho(r)$ = 0.80 × 10^{-2}, 0.81 × 10^{-2}, and 0.68 × 10^{-2} e/a_0^3) and one acetonitrile H atom ($d_{CH\cdots O}$ = 2.395 Å; WBI = 0.004; $\rho(r)$ = 0.87 × 10^{-2} e/a_0^3).

The reactivity *in silico* of receptor **8** was explored toward the hydrogen sulfate (HSO_4^-) anion and the Mg^{2+} cation. Its characteristic electrochemical anodic response (Table 1) is dependent on the relatively high energy of the HOMO (Table 4), which is mainly located at the Fe atom. Reaction with the HSO_4^- anion proceeds preferentially at the concave N(1) side of the receptor (5.92 kcal/mol more stable than at the N(3) side, at the optimization level) leading to anionic complex [**8**·(HSO_4)]$^-$ (see Figure 9a). Besides the two main N−H···O−S

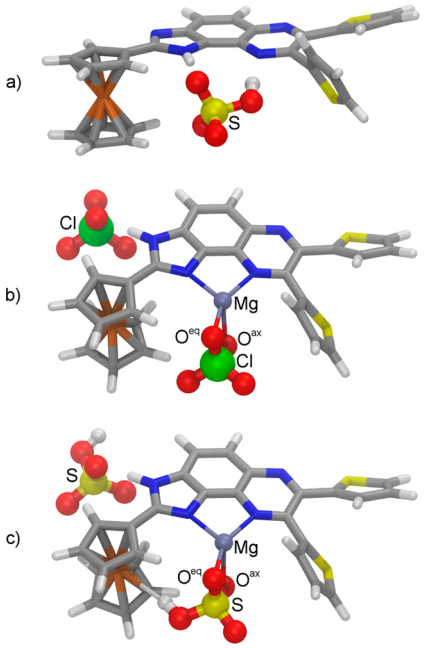

Figure 9. Computed ($COSMO_{MeCN}$/B3LYP-D3/def2-TZVP) most stable geometries for complexes (a) [**8**·(HSO_4)]$^-$, (b) [**8**·$Mg(ClO_4)_2$], and (c) [**8**·$Mg(HSO_4)_2$]. Receptors are displayed as capped sticks, and guest molecule in ball-and-stick representations.

(∠NHO = 175.0°; $d_{NH\cdots O}$ = 1.768 Å; WBI = 0.065; $\rho(r)$ = 4.03 × 10^{-2} e/a_0^3) and SO−H···N(9) (∠NOH = 173.0°; $d_{OH\cdots N}$ = 1.823 Å; WBI = 0.079; $\rho(r)$ = 4.10 × 10^{-2} e/a_0^3) strong hydrogen bonds (HBs), the anion is effectively anchored by three other secondary HBs of the O atoms, within the HSO_4^- moiety, with ferrocenyl H atoms ($d_{O\cdots H}$ = 2.317, 2.681, and 2.730 Å; WBI = 0.005, 0.001 and 0.001; $\rho(r)$ = 1.21 × 10^{-2}, 0.69 × 10^{-2}, and 0.57 × 10^{-2} e/a_0^3). This anion complexation does not significantly change the energy of the HOMO, which is also preferentially located at Fe (see Table 4).

In the case of reaction of **8** with $Mg(ClO_4)_2$, the metal cation is strongly chelated by the imidazole N(1) and pyrazine N(9) donor atoms of the receptor (d_{Mg-N} = 2.065 and 2.124 Å; WBI = 0.092 and 0.077; $\rho(r)$ = 4.54 × 10^{-2} and 4.14 × 10^{-2} e/a_0^3) (Figure 9b). Two perchlorate O atoms occupy the third equatorial position (d_{Mg-O} = 2.040 Å; WBI = 0.071; $\rho(r)$ = 4.16 × 10^{-2} e/a_0^3) and the apical positions (d_{Mg-O} = 2.139 Å; WBI = 0.051; $\rho(r)$ = 3.18 × 10^{-2} e/a_0^3) of a distorted trigonal pyramidal environment around the Mg^{2+} ion. This unusual geometry suggests that this is actually a coordinatively unsaturated species and an additional solvent or water molecule (at least) should be brought to the first coordination sphere (*vide infra*). The anionic unit is held at the opposite side of the imidazole ring by a strong NH···O type HB (∠NHO = 170.8; $d_{NH\cdots O}$ = 1.824 Å; WBI = 0.050; $\rho(r)$ = 3.39 × 10^{-2} e/a_0^3) and three secondary weak HBs between perchlorate O and ferrocenyl H atoms ($d_{O\cdots HCp}$ = 2.503, 2.531, and 2.858 Å; WBI = 0.004, 0.003 and 0.001; $\rho(r)$ = 0.81 × 10^{-2}, 0.80 × 10^{-2}, and 0.42 × 10^{-2} e/a_0^3). The receptor behaves as a mediator in the electron transfer arising upon formal N(3) deprotonation from the anion-bound convex side to the metal ion [Mg-(ClO_4)]$^+$ fragment, but the receptor itself is not significantly affected, with regard to its HOMO energy (Table 4), which agrees with the absence of observable changes in the electrochemical response of the receptor in the presence of the HSO_4^- anion.

According to the computed energetics, the addition of HSO_4^- anions to the preformed [**8**·$Mg(ClO_4)_2$] complex is predicted to occur via initial displacement of the oxoanion at the coordination sphere of the metal, leading to a receptor-separated ion-pair complex of the (ClO_4)-**8**-$Mg(HSO_4)$ type, which, at the optimization level, turns out to be 6.61 kcal/mol more stable that the isomeric complex of the [Mg-(ClO_4)]$^+$$(HSO_4)^-$ ion-pair (see the Supporting Information). A second displacement of perchlorate by the HSO_4^- anion would afford a [**8**·$Mg(HSO_4)_2$] complex (Figure 9c), very much resembling the structural features above-described for [**8**·$Mg(ClO_4)_2$]. Indeed, the more basic anionic HSO_4^- unit is also anchored at the convex side of the receptor by a stronger NH···O bond (∠NHO = 174.1°; $d_{NH\cdots O}$ = 1.737 Å; WBI = 0.069; $\rho(r)$ = 4.24 × 10^{-2} e/a_0^3) and three secondary HBs between perchlorate O and ferrocenyl H atoms ($d_{O\cdots HCp}$ = 2.403, 2.460, and 2.648 Å; WBI = 0.005, 0.004 and 0.002; $\rho(r)$ = 1.06 × 10^{-2}, 0.90 × 10^{-2}, and 0.64 × 10^{-2} e/a_0^3). The Mg^{2+} ion is chelated by the receptor N(1) and N(9) donor sites (d_{Mg-N} = 2.070 and 2.130 Å; WBI = 0.090 and 0.079; $\rho(r)$ = 4.49 × 10^{-2} and 4.08 × 10^{-2} e/a_0^3) and the distorted trigonal pyramidal environment around the Mg^{2+} ion is completed by two perchlorate O atoms at the third equatorial (d_{Mg-O} = 2.036 Å; WBI = 0.070; $\rho(r)$ = 4.28 × 10^{-2} e/a_0^3) and the apical positions (d_{Mg-O} = 2.096 Å; WBI = 0.055; $\rho(r)$ = 3.63 × 10^{-2} e/a_0^3). However, the distinctive structural feature of complex [**8**·$Mg(HSO_4)_2$] is the existence of a markedly acidic OH group belonging to the hydrogen sulfate ligand at the coordination sphere of the Mg^{2+} cation, which is oriented toward the ferrocenyl substituent and protonates its basic Fe atom ($d_{Fe\cdots HO}$ = 2.732 Å; WBI = 0.004; $\rho(r)$ = 1.17 × 10^{-2} e/a_0^3; ε = 8.711). This causes an increase of the electric charge at the ferrocenyl moiety, therefore reducing the HOMO energy (Table 4), in agreement with the experimentally observed significant shift of the oxidation wave (see Figure 2d and Table 1). Again, the rather unusual trigonal pyramidal environment for the four-coordinated Mg^{2+} ion indicates its preference for increasing the coordination number by accepting further donor ligands, such as acetonitrile solvent or water. Because of steric constraints imposed by the close proximity of the thienyl substituent at C(8) of the receptor, there seems to be room for only one such

DOI: 10.1021/acs.inorgchem.5b01071
Inorg. Chem. 2015, 54, 7461−7473

additional ligand; hence, the complex **8**·$Mg(HSO_4)_2(H_2O)$ appears to be a likely candidate for the actual species in the electrochemical solution. This coordinatively saturated species **8**·$Mg(HSO_4)_2(H_2O)$ features the Mg^{2+} ion in a distorted pentacoordinated square pyramidal environment (see Figure 10) with an stronger apical Mg−N bond with N(1) (d_{Mg-N} =

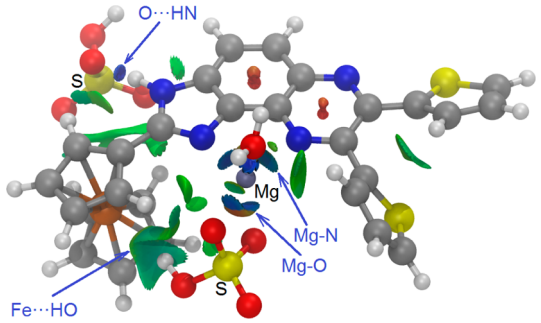

Figure 10. Computed ($COSMO_{MeCN}$/B3LYP-D3/def2-TZVP) most stable structure for complex [**8**·$Mg(HSO_4)_2(H_2O)$] with NCIplot highlighting key stabilizing NCIs; the most significant ones are explicitly indicated with blue arrows and text. The reduced density gradient (RDG) s = 0.3 a.u. isosurface is colored over the range −0.07 a.u. < sign(λ_2)·ρ < 0.07 a.u.[39] [Color legend: blue, strong attraction; green, moderate interaction; and red, strong repulsion.]

2.096 Å; WBI = 0.090; $\rho(r) = 4.20 \times 10^{-2}$ e/a_0^3). The base of the square pyramid is formed by the other N atom of the receptor chelate (d_{Mg-N} = 2.176 Å; WBI = 0.073; $\rho(r) = 3.64 \times 10^{-2}$ e/a_0^3), the two hydrogen sulfate Mg−O bonds (d_{Mg-O} = 2.093 and 2.098 Å; WBI = 0.065 and 0.061; $\rho(r) = 3.63 \times 10^{-2}$ e/a_0^3), and the strongly bound water molecule (d_{Mg-O} = 2.013 Å; WBI = 0.064; $\rho(r) = 4.17 \times 10^{-2}$ e/a_0^3), the later forming an additional HB with a thienyl H atom ($d_{O\cdots H}$ = 2.536 Å; WBI = 0.002; $\rho(r) = 0.86 \times 10^{-2}$ e/a_0^3). Besides the analogous noncovalent interactions (NCIs) also shown for the dehydrated complex (*vide supra*), similar behavior of the H atom in acidic HSO_4^- is observed as it protonates the basic Fe center ($d_{Fe\cdots H}$ = 2.747 Å; WBI = 0.004; $\rho(r) = 1.15 \times 10^{-2}$ e/a_0^3; ε = 2.682), thus causing a significantly low energy for the HOMO (−5.849 eV) mainly located at Fe (66.4%).

These results are in agreement with the perturbations observed in the emission spectrum of these receptors after formation of the above-mentioned ion-pair complexes, which could be rationalized as follows: (i) the weak emission spectrum of **7** or **8** may be explained by a quenching of the imidazoquinoxaline subunit fluorescence by the high-energy lone pair at the Fe atom in the ferrocene moiety; (ii) upon complexation with the metal cation by the action of the lone pairs at the N atoms belonging to the imidazoquinoxaline moiety, the energy of the lone pair at Fe is reduced, partially decreasing its quenching role and therefore a slight enhancement of the fluorescent emission is induced; and (iii) the protonation of the basic Fe center of the ferrocene moiety, in the ion pair, by the H atoms in acidic HSO_4^-, as a result of the addition of this anion to the co-bound metal receptor, induces a reduction in the electron-donating ability in the ferrocene subunit and, consequently, the above-mentioned electron transfer is vanished, leading to a higher fluorescence enhancement.

CONCLUSIONS

The synthesis of tricyclic bis(heteroaryl)-substituted ferrocenyl-imidazo-quinoxalines from readily available 2,3-bis(heteroaryl)-quinoxaline derivative is reported. The presence of redox and fluorescent units at the heteroaromatic core, which is able to behave as ditopic binding framework, converts these molecules in potential candidates to act not only as receptors of simple ionic analytes but also as receptors for the electro-optical recognition of ion pairs. In this context, their binding properties toward several cations and anions, using electrochemical, optical, and spectroscopic techniques, have been studied. Several trends have surfaced from this study, showing different scenarios, which clearly demonstrate the capability of these receptors in the field of the molecular recognition.

(1) Both molecules, which individually had already demonstrated their ability to form the corresponding cationic and anionic complexes, have behaved as ion-pair receptors for cations such as Cd^{2+}, Pb^{2+}, Zn^{2+}, and Hg^{2+}, as well as $H_2PO_4^-$ anions.

(2) Both receptors showed an important increase in their binding ability of the HSO_4^- anion when they were co-bound to cations such as Cd^{2+}, Pb^{2+}, Zn^{2+}, and Hg^{2+}, while the free receptors showed no affinity for this anion. In this case, the emission spectroscopic data revealed that both receptors are able to discriminate HSO_4^- and $H_2PO_4^-$ anions.

(3) Similarly, cations such as Ni^{2+} and Mg^{2+}, which showed no ability to be coordinated by these free receptors, displayed a dramatic increase to be bound when both receptors were complexed with anionic $H_2PO_4^-$ species.

(4) Last, but not least, is the scenario in which the free receptors show a remarkable affinity for binding simultaneously cations, such as Ni^{2+} and Mg^{2+}, and HSO_4^- anions, when in its free form showed no affinity for these ions.

In all of these cases, the ion-pair formation is detected by a perturbation of the redox potential (>200 mV), of the ferrocene moiety, and a remarkable enhancement in the emission band (CHEF = 980).

ASSOCIATED CONTENT

Supporting Information

Supporting information includes general experimental and computational comments; NMR spectra; electrochemical, UV−vis, fluorescence, and ^1H NMR titration data; and Cartesian coordinates for the computed structures. The Supporting Information is available free of charge on the ACS Publications website at DOI: 10.1021/acs.inorgchem.5b01071.

AUTHOR INFORMATION

Corresponding Authors

*E-mail: atarraga@um.es (A. Tarraga).
*E-mail: pmolina@um.es (P. Molina).

Notes

The authors declare no competing financial interest.

ACKNOWLEDGMENTS

We gratefully acknowledge the financial support from MICINN-Spain (Project No. CTQ2011/27175) and Fondo Europeo de Desarrollo Regional (FEDER). One of us (M.A.) also thanks the MICINN for a FPI fellowship.

DOI: 10.1021/acs.inorgchem.5b01071
Inorg. Chem. 2015, 54, 7461−7473

REFERENCES

(1) For very recent overviews of ion pair receptors, see: (a) Kim, S. K.; Sessler, J. L. *Chem. Soc. Rev.* **2010**, *39*, 3784−3809. (b) Gale, P. A. *Coord. Chem. Rev.* **2003**, *240*, 191−221. (c) McConnell, A. J.; Beer, P. D. *Angew. Chem., Int. Ed.* **2012**, *51*, 5052−5061. (d) Molina, P.; Tárraga, A.; Alfonso, M. *Dalton Trans.* **2014**, *43*, 18−29.

(2) (a) Mahoney, J. M.; Beatty, A. M.; Smith, B. D. *J. Am. Chem. Soc.* **2001**, *123*, 5847−5848. (b) Scheerder, J.; van Duynhoven, J. P. M.; Engbersen, J. F. J.; Reinhoudt, D. N. *Angew. Chem., Int. Ed. Engl.* **1996**, *35*, 1090−1093. (c) Custelcean, R.; Delmau, L. H.; Moyer, B. A.; Sessler, J. L.; Cho, W.-S.; Gross, D.; Bates, G. W.; Brooks, S. J.; Light, M. E.; Gale, P. A. *Angew. Chem., Int. Ed.* **2005**, *44*, 2537−2542.

(3) Beer, P. D.; Gale, P. A. *Angew. Chem., Int. Ed.* **2001**, *40*, 486−516.

(4) (a) Lin, T. C.; Lai, C. C.; Chiu, S. H. *Org. Lett.* **2009**, *11*, 613−616. (b) Barrell, M. J.; Leigh, D. A.; Lusby, P. J.; Slawin, A. M. Z. *Angew. Chem., Int. Ed.* **2008**, *47*, 8036−8039. (c) Leontiev, A. V.; Jemmett, C. A.; Beer, P. D. *Chem. - Eur. J.* **2011**, *17*, 816−825.

(5) Niikura, K.; Anslyn, E. V. *J. Org. Chem.* **2003**, *68*, 10156−10157.

(6) For reviews, see: (a) Molina, P.; Tárraga, A.; Caballero, A. *Eur. J. Inorg. Chem.* **2008**, *2008*, 3401−3417. (b) Molina, P.; Tárraga, A.; Alfonso, M. *Eur. J. Org. Chem.* **2011**, *2011*, 4505−4518. (c) Beer, P. D. *Chem. Soc. Rev.* **1989**, *18*, 409−450. (d) Beer, P. D.; Gale, P. A.; Chen, G. Z. *Coord. Chem. Rev.* **1999**, *185−186*, 3−36. (e) Beer, P. D.; Cadman, J. *Coord. Chem. Rev.* **2000**, *205*, 131−155. (f) Beer, P. D.; Hayes, R. J. *Coord. Chem. Rev.* **2003**, *240*, 167−189. (g) Beer, P. D.; Bayly, S. R. *Top. Curr. Chem.* **2005**, *255*, 125−162.

(7) Molina, P.; Tárraga, A.; Otón, F. *Org. Biomol. Chem.* **2012**, *10*, 1711−1724.

(8) For selective sensing of Pb^{2+}, see: (a) Zapata, F.; Caballero, A.; Espinosa, A.; Tárraga, A.; Molina, P. *Org. Lett.* **2008**, *10*, 41−44. (b) Alfonso, M.; Tárraga, A.; Molina, P. *Inorg. Chem.* **2013**, *52*, 7487−7496. For Zn^{2+}, see: (c) Zapata, F.; Caballero, A.; Espinosa, A.; Tárraga, A.; Molina, P. *Org. Lett.* **2007**, *9*, 2385−2388. For Hg^{2+}, see: (d) Alfonso, M.; Contreras-Garcia, J.; Espinosa, A.; Tárraga, A.; Molina, P. *Dalton Trans.* **2012**, *41*, 4437−4444. For AcO^-, see: (f) Sola, A.; Tárraga, A.; Molina, P. *Dalton Trans.* **2012**, *41*, 8401−8509. (g) Sola, A.; Orenes, R. A.; García, M. A.; Claramunt, R. M.; Alkorta, I.; Elguero, J.; Tárraga, A.; Molina, P. *Inorg. Chem.* **2011**, *50*, 4212−4220. For $H_2PO_4^-$, and $HP_2O_7^{3-}$, see: (h) Zapata, F.; Caballero, A.; Tárraga, A.; Molina, P. *J. Org. Chem.* **2010**, *75*, 162−169. (i) Zapata, F.; Caballero; Espinosa; Tárraga, A.; Molina. *J. Org. Chem.* **2008**, *73*, 4034−4044. For ion pair, see: (j) Alfonso, M.; Espinosa, A.; Tárraga, A.; Molina, P. *Org. Lett.* **2011**, *13*, 2078−2081. (k) Alfonso, M.; Tárraga, A.; Molina, P. *Org. Lett.* **2011**, *13*, 6432−6435.

(9) Yamamoto, T.; Sugiyama, K.; Kushida, T.; Inoue, T.; Kanbara, T. *J. Am. Chem. Soc.* **1996**, *118*, 3930−3937.

(10) (a) Black, C. B.; Andrioletti, B.; Try, A. C.; Ruiperez, C.; Sessler, J. L. *J. Am. Chem. Soc.* **1999**, *121*, 10438−10439. (b) Anzenbacher, P., Jr.; Try, A. C.; Miyaji, H.; Jursíková, K.; Lynch, V. M.; Marquez, M.; Sessler, J. L. *J. Am. Chem. Soc.* **2000**, *122*, 10268−10272. (c) Aldakov, D.; Anzenbacher, P., Jr. *Chem. Commun.* **2003**, 1394−1395. (d) Shevchuk, S. V.; Lynch, V. M.; Sessler, J. L. *Tetrahedron* **2004**, *60*, 11283−11291. (e) Ghosh, T.; Maiya, V. G.; Wong, M. W. *J. Phys. Chem. A* **2004**, *108*, 11249−11259. (f) Wang, T.; Bai, Y.; Ma, L.; Yan, X.-P. *Org. Biomol. Chem.* **2008**, *6*, 1751−1755.

(11) (a) Alfonso, M.; Sola, A.; Caballero, A.; Tárraga, A.; Molina, P. *Dalton Trans.* **2009**, 9653−9658. (b) Alfonso, M.; Tárraga, A.; Molina, P. *Dalton Trans.* **2010**, *39*, 8637−8645. (c) Alfonso, M.; Tárraga, A.; Molina, P. *J. Org. Chem.* **2011**, *76*, 939−947.

(12) For a preliminary communication, see: Alfonso, M.; Espinosa, A.; Tárraga, A.; Molina, P. *Chem. Commun.* **2012**, *48*, 6848−6850.

(13) Li^+, K^+, Mg^{2+}, Ni^{2+}, Cd^{2+}, and Pb^{2+} were added as perchlorate salts, while Na^+, Ca^{2+}, Cu^{2+}, Zn^{2+}, and Hg^{2+} were added as triflate salts. ***Caution!*** *Perchlorate derivatives must be handled carefully, because they can cause explosions.*

(14) The OSWV technique has been employed to obtain well-resolved potential information, while the individual redox processes are poorly resolved in the CV experiments in which individual $E_{1/2}$ potentials cannot be easily or accurately extracted from these data: (a) Serr, B. R.; Andersen, K. A.; Elliott, C. M.; Anderson, O. P. *Inorg. Chem.* **1988**, *27*, 4499−4504. (b) Richardson, D. E.; Taube, H. *Inorg. Chem.* **1981**, *20*, 1278−1285.

(15) Specfit/32 Global Analysis System, version 3.0.36 for 32-bit Windows Systems, Spectrum Software Associates, 1999−2004 (SpecSoft@compuserve.com). The Specfit program was acquired from Biologic, SA (www.bio-logic.info) in January 2005. The equation to be adjusted by nonlinear regression, using the above-mentioned software was the following: $\Delta A/b = K_{11}\Delta\varepsilon_{HG}[H]_{tot}[G]/(1 + K_{11}[G])$, where H = host, G = guest, HG = complex, ΔA = variation in the absorption, b = cell width, K_{11} = association constant for a 1:1 model, and $\Delta\varepsilon_{HG}$ = variation of molar absorptivity.

(16) (a) Neese, F. An *ab initio* DFT and semiempirical SCF-MO package, Version 3.02; Max Planck Institute for Bioinorganic Chemistry: Mülheim/Ruhr, Germany, 2012. Web page: http://www.cec.mpg.de/forum/portal.php. (b) Neese, F. *WIREs Comput. Mol. Sci.* **2012**, *2*, 73−78.

(17) (a) Becke, A. D. *J. Chem. Phys.* **1993**, *98*, 5648−5652. (b) Lee, C. T.; Yang, W. T.; Parr, R. G. *Phys. Rev. B: Condens. Matter Mater. Phys.* **1988**, *37*, 785−789.

(18) Neese, F.; Wennmohs, F.; Hansen, A.; Becker, U. *Chem. Phys.* **2009**, *356*, 98−109.

(19) (a) Schäfer, A.; Huber, C.; Ahlrichs, R. *J. Chem. Phys.* **1994**, *100*, 5829−5835. (b) Weigend, F.; Ahlrichs, R. *Phys. Chem. Chem. Phys.* **2005**, *7*, 3297−3305.

(20) Grimme, S.; Antony, J.; Ehrlich, S.; Krieg, H. *J. Chem. Phys.* **2010**, *132*, 154104−154119.

(21) (a) Klamt, A.; Schüürmann, G. *J. Chem. Soc., Perkin Trans. 2* **1993**, *220*, 799−805. (b) Klamt, A. *J. Phys. Chem.* **1995**, *99*, 2224−2235.

(22) Wiberg, K. *Tetrahedron* **1968**, *24*, 1083−1096.

(23) (a) Reed, A. E.; Weinhold, F. *J. Chem. Phys.* **1983**, *78*, 4066−4073. (b) Reed, A. E.; Weinstock, R. B.; Weinhold, F. *J. Chem. Phys.* **1985**, *83*, 735−746 10.1063/1.449486. (c) Glendening, E. D.; Badenhoop, J. K.; Reed, A. E.; Carpenter, J. E.; Bohmann, J. A.; Morales, C. M.; Weinhold, F. *NBO 5.9*; Theoretical Chemistry Institute, University of Wisconsin: Madison, WI, 2001.

(24) (a) Bader, R. F. W. In *Atoms in Molecules: A Quantum Theory*; Oxford University Press: Oxford, U.K., 1990. (b) Bader, R. F. W. *Chem. Rev.* **1991**, *91*, 893−928. (c) Matta, C. F.; Boyd, R. J. In *The Quantum Theory of Atoms in Molecules*; Matta, C. F., Boyd, R. J., Eds.; Wiley−VCH: New York, 2007; pp 1−34.

(25) (a) Biegler-König, F.; Schönbohm, J. *AIM2000, v. 2.0*; 2002. Home page: http://www.aim2000.de/. Biegler-König, F.; Schönbohm, J.; Bayles, D. *J. Comput. Chem.* **2001**, *22*, 545−559. (b) Biegler-König, F.; Schönbohm, J. *J. Comput. Chem.* **2002**, *23*, 1489−1494.

(26) Humphrey, W.; Dalke, A.; Schulten, K. VMD—Visual Molecular Dynamics (v. 1.9.1). *J. Mol. Graphics* **1996**, *14*, 33−38. Home page: http://www.ks.uiuc.edu/Research/vmd/.10.1016/0263-7855(96)00018-5

(27) Ji, J.; Lee, K.-I. *J. Korean Chem. Soc.* **2005**, *49*, 150−154.

(28) Pagoria, P. F.; Mitchell, A. R.; Schmidt, R. D. *J. Org. Chem.* **1996**, *61*, 2934−2935.

(29) Several examples showing the ferrocene oxidation by the action of Cu^{2+} metal cation have been reported; see: (a) Sato, M.; Katada, M.; Nakashima, S.; Sano, H.; Akabori, S. *J. Chem. Soc., Dalton Trans.* **1990**, 1979−1984. (b) Connelly, N. G.; Geiger, W. E. *Chem. Rev.* **1996**, *96*, 877−910. (c) Plenio, H.; Aberle, C.; Al Shihadeh, Y.; Lloris, J. M.; Martínez-Máñez, R.; Pardo, T.; Soto, J. *Chem. - Eur. J.* **2001**, *7*, 2848−2861. (d) Evans, A. J.; Watkins, S. E.; Craig, C.; Colbran, S. B. *J. Chem. Soc., Dalton Trans.* **2002**, 983−994.

(30) (a) Otón, F.; Tárraga, A.; Espinosa, A.; Velasco, M. D.; Molina, P. *Dalton Trans* **2006**, 3685−3692. (b) Caballero, A.; Espinosa, A.; Tárraga, A.; Molina, P. *J. Org. Chem.* **2008**, *73*, 5489−5497. (c) Romero, T.; Caballero, A.; Espinosa, A.; Tárraga, A.; Molina, P. *Dalton Trans.* **2009**, 2121−2129. (d) Zapata, F.; Caballero, A.;

DOI: 10.1021/acs.inorgchem.5b01071
Inorg. Chem. 2015, 54, 7461−7473

Espinosa, A.; Tárraga, A.; Molina, P. *Inorg. Chem.* **2009**, *48*, 11566−11575.
(31) One way to reveal the formation of hydrogen-bonded complexes under conditions of electrochemical titrations is to suppress deprotonation by adding a small amount of acetic acid; see: Alfonso, M.; Tárraga, A.; Molina, P. *J. Org. Chem.* **2011**, *76*, 939−947.
(32) The addition of increasing amounts of F^- anion to receptors **7** and **8** gave rise to a remarkable cathodic shift of their oxidation peaks (Figure S41 in the Supporting Information). However, when the titration was performed in the presence of 20 equiv of AcOH, no electrochemical response was noticed. Moreover, upon titration of the free receptors with a strong base, such as Bu_4NOH, which only induced a deprotonation process, the same cathodic shifts of the oxidation peaks were observed ($\Delta E_{1/2} = -305$ mV) for both receptors (Figure S42 in the Supporting Information).
(33) (a) Lankshear, M. D.; Cowley, A. R.; Beer, P. D. *Chem. Commun.* **2006**, 612−614. (b) Lankshear, M. D.; Dudley, I. M.; Chan, K.-M.; Cowley, A. R.; Santos, S. M.; Felix, V.; Beer, P. D. *Chem.—Eur. J.* **2008**, *14*, 2248−2263.
(34) Shortreed, M.; Kopelman, R.; Kuhn, M.; Hoyland, B. *Anal. Chem.* **1996**, *68*, 1414−1418.
(35) Begg, S. L.; Eijkelkamp, B. A.; Luo, Z.; Couñago, R. M.; Morey, J. R.; Maher, M. J.; Ong, C-I. Y.; McEwan, A. G.; Kobe, B.; O'Mara, M. L.; Paton, J. C.; McDevitt, C. A. *Nat. Commun.* **2015**, *6*, 6418−6428.
(36) For the behavior towards hydrogen sulfate, see ref 8j and the Supporting Information.
(37) Shimoni-Livny, L.; Glusker, J. P.; Bock, C. W. *Inorg. Chem.* **1998**, *37*, 1853−1867.
(38) (a) Hancock, R. D.; Salim Shaikjee, M.; Dobson, S. M.; Boeyens, J. C. A. *Inorg. Chim. Acta* **1988**, *154*, 229−238. (b) Hancock, R. D.; Reibenspies, J. H.; Maumela, H. *Inorg. Chem.* **2004**, *43*, 2981−2987. (c) Gephart, R. T., III; Williams, N. J.; Reibenspies, J. H.; De Sousa, A. S.; Hancock, R. D. *Inorg. Chem.* **2008**, *47*, 10342−10348. (d) Sola, A.; Espinosa, A.; Tárraga, A.; Molina, P. *Sensors* **2014**, *14*, 14339−14355.
(39) (a) Johnson, E. R.; Keinan, S.; Mori-Sánchez, P.; Contreras García, J.; Cohen, A. J.; Yang, W. *J. Am. Chem. Soc.* **2010**, *132*, 6498−6506. (b) Contreras García, J.; Johnson, E. R.; Keinan, S.; Chaudret, R.; Piquemal, J.-P.; Beratan, D. N.; Yang, W. *J. Chem. Theory Comput.* **2011**, *7*, 625−632. (c) *NCIplot, Version 1.1.2*; Department of Chemistry, Duke University: Durham, NC, 2011. Available via the Internet at: http://www.chem.duke.edu/~yang/Software/softwareNCI.html.

DOI: 10.1021/acs.inorgchem.5b01071
Inorg. Chem. 2015, 54, 7461−7473